

This Page Is Inserted by IFW Operations  
and is not a part of the Official Record

## **BEST AVAILABLE IMAGES**

Defective images within this document are accurate representations of the original documents submitted by the applicant.

Defects in the images may include (but are not limited to):

- BLACK BORDERS
- TEXT CUT OFF AT TOP, BOTTOM OR SIDES
- FADED TEXT
- ILLEGIBLE TEXT
- SKEWED/SLANTED IMAGES
- COLORED PHOTOS
- BLACK OR VERY BLACK AND WHITE DARK PHOTOS
- GRAY SCALE DOCUMENTS

**IMAGES ARE BEST AVAILABLE COPY.**

**As rescanning documents *will not* correct images,  
please do not report the images to the  
Image Problem Mailbox.**

APPLICATION  
FOR  
UNITED STATES LETTERS PATENT

TITLE: ALKALINE BATTERY

APPLICANT: WILLIAM L. BOWDEN, KLAUS BRANDT AND PAUL A.  
CHRISTIAN

CERTIFICATE OF MAILING BY EXPRESS MAIL

Express Mail Label No. EL 983 021 898 US

March 9, 2004

Date of Deposit

# ALKALINE BATTERY

## TECHNICAL FIELD

This invention relates to an alkaline battery and a method of manufacturing an alkaline battery.

## BACKGROUND

5        Batteries, such as alkaline batteries, are commonly used as energy sources. Generally, alkaline batteries have a cathode, an anode, a separator and an alkaline electrolyte solution. The cathode can include a cathode material (e.g., manganese dioxide or nickel oxyhydroxide), carbon particles that enhance the conductivity of the cathode, and a binder. The anode can be formed of a gel including zinc particles. The separator is disposed between the cathode and the anode. The 10      alkaline electrolyte solution, which is dispersed throughout the battery, can be an aqueous hydroxide solution such as potassium hydroxide.

## SUMMARY

An alkaline battery includes a cathode including a manganese dioxide having a spinel-type crystal structure (e.g.,  $\lambda$ -MnO<sub>2</sub>) and an anode including zinc. The alkaline battery can have 15      an average closed circuit voltage of about 1.3V at low rates of discharge, adequate high-rate performance, and sufficient capacity retention when stored. The lambda-manganese dioxide can have a specific discharge capacity at low-rate (e.g., C/30 or 10 mA/g of active cathode material) to a 0.8V cutoff of greater than 310 mAh/g. An average closed circuit voltage of at least about 1.3V can provide voltage compatibility with commercial manganese dioxide-zinc primary 20      alkaline batteries.

In one aspect, an alkaline battery includes a cathode including an active cathode material including lambda-manganese dioxide, an anode including zinc, a separator between the anode and the cathode, and an alkaline electrolyte contacting the anode and the cathode. The active cathode material has a specific discharge capacity to a 0.8V cutoff of greater than 290 mAh/g, 25      greater than 300 mAh/g, greater than 310 mAh/g, or greater than 320 mAh/g, at a discharge rate corresponding to 20 mA/g or 10 mA/g of active cathode material.

In another aspect, a method of manufacturing an alkaline battery includes providing a positive electrode including an active cathode material including lambda-manganese oxide, and

5 forming a battery including the electrode and a negative electrode including zinc particles. Providing the electrode includes preparing lambda-manganese dioxide by contacting water with a compound of the formula  $Li_{1+x}Mn_{2-x}O_4$ , wherein  $x$  is from -0.02 to +0.02 or from -0.005 to +0.005, adding an acid to the water and the compound to form a mixture until the mixture has a pH of 1 or less, separating a solid from the water and acid, and drying the solid, optionally *in vacuo*, at a temperature of 150°C or below to obtain the lambda-manganese dioxide. The alkaline battery has a specific discharge capacity to a 0.8V cutoff of greater than 300 mAh/g at a discharge rate corresponding to 10 mA/g active cathode material.

10 The lambda-manganese dioxide can have a B.E.T. surface area of between 1 and 10  $m^2/g$  (e.g., greater than 8  $m^2/g$ ), a total pore volume of between 0.05 and 0.15 cubic centimeters per gram (e.g., 0.05 to 0.15 cubic centimeters per gram), or an average pore size of less than 100 Å. The acid can be sulfuric acid, nitric acid, perchloric acid, hydrochloric acid, toluene sulfonic acid, or trifluoromethyl sulfonic acid. Concentration of acid can be between 1 and 8 molar. The final pH can be 1 or less, 0.7 or less, or between 0.5 and 0.7. The method can include washing the solid separated from the water and acid with water until the washings have a pH of between 6 15 and 7.

The solid can be dried at a temperature between 20°C and 120°C, between 30°C to 90°C, or between 50°C and 70°C.

20 Contacting water and the compound can include forming a slurry. The slurry can be maintained at a temperature between about 5°C and 50°C. The temperature of the slurry can be maintained substantially constant during the addition of acid.

Other features and advantages of the invention will be apparent from the description and drawings, and from the claims.

#### DESCRIPTION OF DRAWINGS

25 Figure 1 is a cross-section view of a battery.

Figure 2 is a graph depicting a comparison of x-ray powder diffraction patterns for  $\lambda$ -MnO<sub>2</sub> powders prepared from a stoichiometric LiMn<sub>2</sub>O<sub>4</sub> spinel precursor.

30 Figure 3 is a graph depicting the discharge performance of alkaline button cells with cathodes containing either  $\lambda$ -MnO<sub>2</sub> or a commercial electrolytic manganese dioxide (EMD) discharged at a rate of C/30 or 10 mA/g of active cathode material to a 0.6V cutoff.

Figure 4 is a graph depicting the incremental discharge capacity and maximum power, determined by Stepped Potential Electro-Chemical Spectroscopy (SPECS) for an alkaline button cell having a cathode including  $\lambda$ -MnO<sub>2</sub>.

5 Figure 5 is a graph depicting the incremental discharge capacity and maximum power, determined by Stepped Potential Electro-Chemical Spectroscopy (SPECS) for an alkaline button cell having a cathode including a commercial EMD.

#### DETAILED DESCRIPTION

Referring to the Figure 1, battery 10 includes a cathode 12 (positive electrode), an anode 14 (negative electrode), a separator 16 and a cylindrical housing 18. Battery 10 also includes 10 current collector 20, seal 22, and a negative metal top cap 24, which serves as the negative terminal for the battery. The cathode is in contact with the housing, and the positive terminal of the battery is at the opposite end of the battery from the negative terminal. An electrolytic solution is dispersed throughout battery 10. Battery 10 can be, for example, an AA, AAA, AAAA, C, or D battery.

15 Anode 14 can be formed of any of the standard zinc materials used in battery anodes. For example, anode 14 can be a zinc slurry that can include zinc metal particles, a gelling agent, and minor amounts of additives, such as a gassing inhibitor. In addition, a portion of the electrolyte solution can be dispersed throughout the anode.

The zinc particles can be any of the zinc particles conventionally used in slurry anodes. 20 Examples of zinc particles can include those described in U.S. Appln. No. 08/905,254, U.S. Appln. No. 09/115,867, or U.S. Appln. No. 09/156,915, each of which is hereby incorporated by reference in its entirety. The anode can include, for example, between 60 wt % and 80 wt %, between 65 wt % and 75 wt %, or between 67 wt % and 71 wt % of zinc particles.

The electrolyte can be an aqueous solution of alkali hydroxide, such as potassium 25 hydroxide or sodium hydroxide. The electrolyte can contain between 15 wt % and 60 wt %, between 20 wt % and 55 wt %, or between 30 wt % and 50 wt % alkali hydroxide dissolved in water. The electrolyte can contain 0 wt % to 6 wt % alkali oxide, such as zinc oxide.

Examples of a gelling agent can include a polyacrylic acid, a grafted starch material, a 30 salt of a polyacrylic acid, a carboxymethylcellulose, a salt of a carboxymethylcellulose (e.g., sodium carboxymethylcellulose) or combinations thereof. Examples of a polyacrylic acid

includes CARBOPOL 940 and 934 (available from B.F. Goodrich) and POLYGEL 4P (available from 3V), and an example of a grafted starch material includes WATERLOCK A221 or A220 (available from Grain Processing Corporation, Muscatine, IA). An example of a salt of a polyacrylic acid includes ALCOSORB G1 (available from Ciba Specialties). The anode can 5 include, for example, between, between 0.05 wt % and 2 wt %, or between 0.1 wt % and 1 wt % gelling agent.

A gassing inhibitor can include an inorganic material, such as bismuth, tin, or indium. Alternatively, a gassing inhibitor can include an organic compound, such as a phosphate ester, an 10 ionic surfactant or a nonionic surfactant. Examples of ionic surfactants are disclosed in, for example, U.S. Patent No. 4,777,100, which is hereby incorporated by reference in its entirety.

Separator 16 can be a conventional battery separator. In some embodiments, separator 16 can be formed of two layers of non-woven, non-membrane material with one layer being disposed along a surface of the other. For example, to minimize the volume of separator 16 while providing an efficient battery, each layer of non-woven, non-membrane material can have 15 a basic weight of about 54 grams per square meter, a thickness of about 5.4 mils when dry and a thickness of about 10 mils when wet. The layers can be substantially devoid of fillers, such as inorganic particles.

In other embodiments, separator 16 can include a layer of cellophane combined with a 20 layer of non-woven material. The separator also can include an additional layer of non-woven material. The cellophane layer can be adjacent cathode 12 or the anode. The non-woven material can contain from 78 wt % to 82 wt % polyvinyl alcohol and from 18 wt % to 22 wt % rayon with a trace amount of a surfactant, such as non-woven material available from PDM under the trade name PA25.

Housing 18 can be a conventional housing commonly used in primary alkaline batteries. 25 The housing can include an inner metal wall and an outer electrically non-conductive material such as a heat shrinkable plastic. Optionally, a layer of conductive material can be disposed between the inner wall and cathode 12. The layer can be disposed along the inner surface of the inner wall, along the circumference of cathode 12, or both. The conductive layer can be formed, for example, of a carbonaceous material (e.g., colloidal graphite), such as LB1000 (Timcal), 30 Eccocoat 257 (W.R. Grace & Co.), Electrodag 109 (Acheson Colloids Company), Electrodag EB-009 (Acheson), Electrodag 112 (Acheson) and EB0005 (Acheson). Methods of applying the

conductive layer are disclosed in, for example, Canadian Patent No. 1,263,697, which is hereby incorporated by reference in its entirety.

Current collector 28 can be made from a suitable metal, such as brass. Seal 30 can be made, for example, of a nylon.

5 Cathode 12 includes an active cathode material and conductive carbon particles.

Optionally, cathode 12 can also include an oxidative additive, or a binder, or both. Generally, the cathode can include, for example, between 60% by weight and 97% by weight, between 80% by weight and 95% by weight, or between 85% by weight and 90% by weight of cathode material.

10 The conductive carbon particles can include graphite particles. The graphite particles can be synthetic graphite particles, including expanded graphite, non-synthetic, or natural graphite, or a blend thereof. Suitable graphite particles can be obtained from, for example, Brazilian Nacional de Grafite of Itapecerica, MG Brazil (e.g., NdG grade MP-0702X) Chuetsu Graphite Works, Ltd. (e.g., Chuetsu grades WH-20A and WH-20AF) of Japan or Timcal America of Westlake, Ohio (e.g., Timcal grade EBNB-90). The cathode can include, for example, between 15 2 wt% and 35 wt%, between 3 wt % and 10 wt%, or between 4 wt % and 8 wt % of carbon particles or blend of carbon particles.

20 Examples of binders can include a polymer such as polyethylene, polyacrylamide, or a fluorocarbon resin, such as PVDF or PTFE. An example of a polyethylene binder is sold under the trade name COATHYLENE HA-1681 (available from Hoechst). The cathode can include, for example, between 0.05 wt % and 5 wt %, or between 0.1 wt % and 2 wt % binder.

A portion of the electrolyte solution can be dispersed through cathode 12, and the weight percentages provided above and below are determined after the electrolyte solution has been dispersed.

25 The cathode material includes lambda-manganese dioxide ( $\lambda\text{-MnO}_2$ ), which can be synthesized by an oxidative delithiation process from a lithium manganese oxide spinel precursor prepared by various synthetic methods and having a general composition  $\text{LiMn}_2\text{O}_4$  and specific physical properties. A suitable lithium manganese oxide spinel precursor can be prepared as described in, for example, U.S. Patent Nos. 4,246,253, 4,507,371, 4,828,834, 5,245,932, 30 5,425,932, 5,997,839, or 6,207,129, each of which is incorporated by reference in its entirety. More particularly, a lithium manganese oxide spinel precursor can have a formula of

$\text{Li}_{1+x}\text{Mn}_{2-x}\text{O}_4$ , where x is between -0.05 and +0.05, preferably between -0.02 and +0.02, more preferably between -0.005 and +0.005. Alternatively, lithium manganese oxide spinel can be obtained, for example, from Kerr-McGee Chemical Company, (Oklahoma City, Oklahoma), or Carus Chemical Company, (Peru, Illinois).

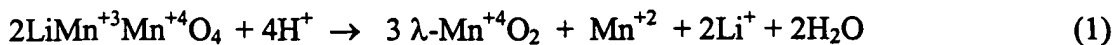
5 Physical, microstructural, and chemical properties for some commercial samples of  $\text{LiMn}_2\text{O}_4$ -type spinels obtained from several suppliers are summarized in Table 1. The x-ray powder diffraction (XRD) patterns for the  $\text{LiMn}_2\text{O}_4$ -type spinel powders were measured using a Rigaku Miniflex diffractometer using  $\text{Cu K}_\alpha$  radiation. The spinel powder from Carus Chemical (Spinel B) has the largest refined cubic lattice cell constant,  $a_0$ , and also has a chemical 10 composition very close to that for stoichiometric  $\text{LiMn}_2\text{O}_4$  spinel. The reported (e.g., ICDD PDF No. 35-0782) cubic lattice constant for stoichiometric spinel is 8.248 Å. The other spinel  $\text{LiMn}_2\text{O}_4$  powder from Kerr-McGee (Spinel A) has an XRD powder diffraction pattern that gives a refined lattice constant of 8.231 Å. This  $a_0$  value is more consistent with those values typically reported for spinels having a slight excess lithium stoichiometry (i.e.,  $\text{Li}_{1+x}\text{Mn}_{2-x}\text{O}_4$ , where x is 15 between 0.005 and 0.1). The  $a_0$  values for such spinels decrease linearly as x increases for x values between -0.15 and 0.25. See, for example, U. S. Patent No. 5,425,932, which is incorporated by reference in its entirety.

The oxidative delithiation process can include, for example, the following steps:

- 20 1. A slurry of the precursor spinel powder is formed with stirring in distilled or deionized water and adjusted to a temperature between about 10 and 50°C, preferably between about 15°C and 30°C;
- 25 2. An aqueous solution of an acid, such as, for example, sulfuric acid, nitric acid, hydrochloric acid, perchloric acid, toluenesulfonic acid or trifluoromethylsulfonic acid, is added to the slurry with constant stirring at a rate to maintain a constant slurry temperature until the pH of the slurry stabilizes at a value typically below about 2, below about 1, or below about 0.7, but greater than about 0.5, and remains constant at this value for at least 0.75 hour (optionally, stirring can be continued for up to an additional 24 hours);
- 30 3. The solid product is separated from the supernatant liquid, for example, by suction, pressure filtration, or centrifugation, and is washed with aliquots of distilled or deionized water until the washings have a neutral pH (e.g., between about 6-7); and

4. The solid product is dried *in vacuo* for between 4 and 24 hours at 30 to 120°C, or at 50 to 90°C, or at 60°C to 70°C.

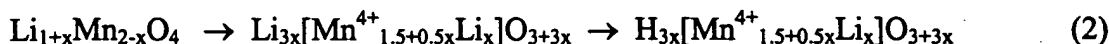
After processing, the dried solid typically exhibits a weight loss of about 25 wt% relative to the initial weight of the precursor LiMn<sub>2</sub>O<sub>4</sub> spinel powder. The total lithium content of the 5 stoichiometric LiMn<sub>2</sub>O<sub>4</sub> spinel is about 4.3 wt%. The observed weight loss can be attributed to the dissolution of lithium ions that migrated to the surface of the spinel particles as well as Mn<sup>+2</sup> ions from the LiMn<sub>2</sub>O<sub>4</sub> spinel crystal lattice putatively resulting from a disproportionation reaction whereby Mn<sup>+3</sup> ions on the surface of the spinel particles are converted to insoluble Mn<sup>+4</sup> ions that remain on the surface and soluble Mn<sup>+2</sup> ions that dissolve in the acid solution according 10 to Equation 1:



The x-ray diffraction patterns for the  $\lambda$ -MnO<sub>2</sub> powders were measured using a Rigaku Miniflex diffractometer using Cu K $\alpha$  radiation. The XRD powder patterns for the various dried  $\lambda$ -MnO<sub>2</sub> powders are consistent with that pattern reported for  $\lambda$ -MnO<sub>2</sub> (e.g., ICDD PDF No. 44-0992). See, U.S. Patent No. 4,246,253, which is incorporated by reference in its entirety. The 15 lattice constants,  $a_0$ , for the refined cubic unit cells for the samples of  $\lambda$ -MnO<sub>2</sub> prepared by the method described above are given in Table 1. The  $a_0$  values range between 8.035 and 8.048 Å. Figure 2 is a graph depicting a comparison of x-ray powder diffraction patterns for  $\lambda$ -MnO<sub>2</sub> powders prepared by either 0.75 or 16 hours of acid treatment of a precursor spinel and the 20 corresponding precursor spinel powder from Kerr-McGee having a nominal excess lithium stoichiometry of Li<sub>1.05</sub>Mn<sub>1.95</sub>O<sub>4</sub>. The XRD powder pattern for  $\lambda$ -MnO<sub>2</sub> is distinguishable from that for the corresponding precursor spinel as shown in Figure 2 for a sample of precursor spinel having a nominal excess lithium stoichiometry of Li<sub>1.05</sub>Mn<sub>1.95</sub>O<sub>4</sub> and the corresponding  $\lambda$ -MnO<sub>2</sub> acid-treated for either 0.75 or 16 hours by the shift in the positions of the diffraction peaks of the 25 precursor spinel to higher 2 $\theta$  angles for the  $\lambda$ -MnO<sub>2</sub>.

The precursor spinel can have a nominally stoichiometric composition, for example, a composition having the general formula Li<sub>1+x</sub>Mn<sub>2-x</sub>O<sub>4</sub>, wherein x is from -0.02 to +0.02, such as Li<sub>1.01</sub>Mn<sub>1.99</sub>O<sub>4</sub>, from which more complete delithiation can be accomplished, and in general, replacement of the lithium ions with protons by an ion-exchange reaction according to equation 2 30 can be reduced or avoided. It is thought that the presence of protons in lattice sites formerly

occupied by the lithium ions can result in thermal instability and decreased discharge capacities for alkaline cells having cathodes including such materials.



where  $0.02 < x < 0.33$

5

Specific surface areas of the various  $\lambda$ - $\text{MnO}_2$  powders as determined by multipoint nitrogen adsorption isotherms by the B.E.T. method as described by P. W. Atkins in "Physical Chemistry", 5<sup>th</sup> ed., New Your: W. H. Freeman & Co., 1994, pp. 990-2. B.E.T. surface area measurements were found to be substantially greater than those for the corresponding precursor spinel powders. See, Table 1. This increase in surface area is consistent with apparent increased roughness or porosity in the surface microstructure of the particles observed by comparing SEM micrographs (10,000X) of particles of the precursor spinel, for example, and particles of the corresponding  $\lambda$ - $\text{MnO}_2$ . Further, porosimetric measurements on a precursor spinel powder and the corresponding  $\lambda$ - $\text{MnO}_2$  powder revealed that the total pore volume more than doubled after de-lithiation to  $\lambda$ - $\text{MnO}_2$  and that the average pore size decreased by nearly 80%.

10

15

Table 1

Precursor Spinel	Spinel A	Spinel B
Lattice constant, $a_0$ Spinel (Å)	8.231	8.242
Lattice constant, $a_0$ $\lambda$ - $\text{MnO}_2$ (Å)	8.048	8.035
B.E.T. SSA, Spinel (m <sup>2</sup> /g)	0.44	3.43
B.E.T. SSA, $\lambda$ - $\text{MnO}_2$ (m <sup>2</sup> /g)	4.98	8.30
Average particle size, Spinel (μm)	12	14.6
Average Pore Size, Spinel (Å)		157
Average Pore Size, $\lambda$ - $\text{MnO}_2$ (Å)		36.5
Total Pore Volume, Spinel (cc/g)		0.05
$\lambda$ - $\text{MnO}_2$ Total Pore Volume (cc/g)		0.11
Tap Density, Spinel (g/cm <sup>3</sup> )	2.10	2.08
True Density, Spinel (g/cm <sup>3</sup> )	4.225	4.196
True Density, $\lambda$ - $\text{MnO}_2$ (g/cm <sup>3</sup> )	4.480	4.442
Spinel Stoichiometry, $\text{Li}_{1+x}\text{Mn}_{2-x}\text{O}_4$ , $x = ?$	0.06-0.08	0.01

20

In certain embodiments, precursor spinels that permit preparation of  $\lambda$ - $\text{MnO}_2$  in accordance with the present invention can be selected according to the following selection criteria: (1) general chemical formula is  $\text{Li}_{1+x}\text{Mn}_{2-x}\text{O}_4$  wherein  $x$  ranges from -0.05 to +0.05, preferably from -0.02 to +0.02, more preferably from -0.005 to +0.005; (2) B.E.T. surface area

of the precursor spinel powder is between about 2 and 10 m<sup>2</sup>/g; (3) total pore volume of the precursor spinel powder is between about 0.02 and 0.1 cubic centimeters per gram; and (4) average pore size of the precursor spinel powder is between about 100 and 300 Å.

The thermal stability of the  $\lambda$ -MnO<sub>2</sub> powder prepared from Spinel B as described above  
5 was evaluated in order to determine the effects of various thermal treatments during cathode  
fabrication (e.g., drying, coating, pressing, etc.) on cell discharge performance. The XRD  
powder patterns for a sample of  $\lambda$ -MnO<sub>2</sub> powder heated *in vacuo* at 120°C for 4 hours was found  
to be identical to that for a bulk sample of  $\lambda$ -MnO<sub>2</sub> powder originally dried *in vacuo* at 70°C for  
up to 16 hours, indicating adequate thermal stability at this temperature. The XRD powder  
10 pattern for a sample of  $\lambda$ -MnO<sub>2</sub> powder heated *in vacuo* at 150°C for 4 hours exhibited a slight  
broadening of the  $\lambda$ -MnO<sub>2</sub> peaks as well as the appearance of a new broad peak at a 2θ angle of  
about 20° indicating the onset of decomposition of the  $\lambda$ -MnO<sub>2</sub> phase. Heating a sample of  $\lambda$ -  
15 MnO<sub>2</sub> powder *in vacuo* at 180°C for 4 hours resulted in the complete disappearance of the  
characteristic  $\lambda$ -MnO<sub>2</sub> peaks and the appearance of several broad peaks in the XRD pattern  
suggesting the formation of one or more new phases. These poorly resolved new peaks can be  
attributed to the presence of  $\beta$ -MnO<sub>2</sub> and  $\epsilon$ -MnO<sub>2</sub> phases.

In addition to evaluating the thermal stability of the  $\lambda$ -MnO<sub>2</sub> powder, the thermal stability  
of  $\lambda$ -MnO<sub>2</sub> in pressed composite cathodes containing conductive carbon particles and a binder  
was evaluated. XRD patterns for pressed composite cathodes heated for 4 hours at 120°C  
20 showed a broadening of the  $\lambda$ -MnO<sub>2</sub> peaks as well as the appearance of several new, broad, weak  
peaks attributed to the  $\epsilon$ -MnO<sub>2</sub> phase indicating the onset of decomposition of the  $\lambda$ -MnO<sub>2</sub> phase.  
Thus,  $\lambda$ -MnO<sub>2</sub> in the pressed composite cathode appears to start decomposing at an even lower  
temperature than  $\lambda$ -MnO<sub>2</sub> powder alone. In XRD patterns for cathodes heated at 150°C or  
180°C, all of the peaks attributed to the  $\lambda$ -MnO<sub>2</sub> phase disappeared completely, and only broad  
25 peaks characteristic of the  $\epsilon$ -MnO<sub>2</sub> phase were present. Furthermore, unlike the case of  $\lambda$ -MnO<sub>2</sub>  
powder, no peaks for the  $\beta$ -MnO<sub>2</sub> phase could be discerned in the XRD pattern for a composite  
cathode heated at 180°C.

Batteries (button cells) including lambda-manganese dioxide in the cathode were  
prepared according to the following examples.

EXAMPLE 1

A sample of dried  $\lambda$ -MnO<sub>2</sub> powder was prepared as follows. Approximately 120 g of Spinel B, a nearly stoichiometric lithium manganese oxide spinel having a nominal composition of Li<sub>1.01</sub>Mn<sub>1.99</sub>O<sub>4</sub> (Carus Chemical Co.), was added with stirring to about 200 ml distilled water to form an aqueous slurry that was cooled to 15°C. 6M H<sub>2</sub>SO<sub>4</sub> was added dropwise with constant stirring until the pH of the slurry stabilized at about 0.7. The slurry was stirred for an additional 20 hours at pH 0.7. The rate of acid addition was adjusted so as to maintain the temperature of the slurry at 15°C. The solid was separated from the liquid by either pressure or suction filtration through a non-woven, spun-bonded polyethylene film (Dupont, Tyvek) and washed with aliquots of distilled water until the washings had a neutral pH (e.g., a pH of about 6). The solid filtercake was dried *in vacuo* for 4-16 hours at 70°C. The weight of the dried  $\lambda$ -MnO<sub>2</sub> product was about 87 g, which corresponds to a weight loss of about 27.5%.

The  $\lambda$ -MnO<sub>2</sub> powder was blended manually using a mortar and pestle with natural graphite (Nacionale de Grafite, MP-0702X) and KOH electrolyte solution containing 38 wt% KOH and 2 wt% zinc oxide in a weight ratio of 60:35:5. About 0.5 g of this cathode mixture was pressed into a nickel wire grid welded to the bottom of a cathode can of a 635-type alkaline button cell. A polymeric insulating seal was inserted into the cathode can. A separator sheet in the form of a disk was saturated with electrolyte solution and placed on top of the cathode disk. Additional electrolyte solution was added by the application of a vacuum so that the electrolyte solution fully penetrated the separator sheet and wetted the cathode. A layer of anode mixture containing particulate zinc, electrolyte, and gelling agent was applied to the upper surface of the separator sheet. The anode can cover was positioned on top of the cell assembly and mechanically crimped to hermetically seal the cell.

The open circuit voltages for freshly assembled cells were measured and are given in Table 2. The cells were discharged at several different constant currents including 30 mA, 6 mA, and 3 mA, nominally corresponding to C/30, C/15 and C/3 discharge rates for Examples 1a, 1b and 1c, respectively. For example, a C/30 rate corresponds to that discharge rate at which the cell capacity was discharged in a period of 30 hours. The C/30, C/15, and C/3 discharge rates further correspond to 10 mA/g, 20mA/g and 100 mA/g of active cathode material. The gravimetric discharge capacities for cells discharged continuously at each of the constant currents to cutoff voltages of 1V and 0.8V also are given in Table 2. The values of capacities to

0.8V obtained for the C/30 and C/15 rates were quite similar but were about 10 to 15% greater than those obtained for comparable cells having cathodes containing EMD (see Comparative Example 1) instead of  $\lambda$ -MnO<sub>2</sub> and discharged at corresponding rates as shown in Figure 3.

#### COMPARATIVE EXAMPLE 1

5 EMD (Kerr-McGee, Trona D) powder was blended manually using a mortar and pestle with natural graphite (Nacionale de Grafite, MP-0702X) and 38% KOH electrolyte solution in a weight ratio of 60:35:5. About 0.5 g of this cathode mix was pressed into a cathode disk in the bottom of the cathode can of a 635-type alkaline button cell. Button cell assembly was completed as described in Example 1. The open circuit voltages for freshly assembled cells were 10 measured and are given in Table 2. The cells were discharged at several different constant currents including 30 mA, 6 mA, and 3 mA, nominally corresponding to C/3, C/15 and C/30 discharge rates, respectively. The gravimetric discharge capacities for cells discharged at each of the above constant currents to cutoff voltages of 1V and 0.8V are given in Table 2. Discharge capacities to 0.8V of 282 mAh/g and 266 mAh/g were obtained for button cells discharged at 15 C/30 (Figure 10) and C/15 rates, respectively. However, cells discharged at the C/3 rate to a 0.8V cutoff gave considerably lower capacities of 215 mAh/g.

20 The averaged discharge curve for cells of Example 1 discharged at a C/30 rate is compared with the corresponding curve for cells of Comparative Example 2 having cathodes containing commercial EMD (e.g., Kerr-McGee, "Trona D") in Figure 3. The profiles of the discharge curves for cells with cathodes containing  $\lambda$ -MnO<sub>2</sub> exhibit an elongated discharge 25 plateau at about 0.95 to 1V that can be attributed to the reduction of Mn<sup>+3</sup> ions by a second electron to Mn<sup>+2</sup>.

#### COMPARATIVE EXAMPLE 2

25 A sample of dried  $\lambda$ -MnO<sub>2</sub> powder was prepared as described in Example 1, but with Spinel A (Kerr-McGee, Grade LMO-210) substituted for Spinel B. The  $\lambda$ -MnO<sub>2</sub> powder was blended either manually using a mortar and pestle or mechanically using a high-speed laboratory mixer mill (e.g., Waring mixer) with natural graphite (Nacionale de Grafite, MP-0702X) and 38% KOH electrolyte solution in a weight ratio of 60:35:5.

30 Button cells having cathodes containing this cathode mix were fabricated in the same manner as in Example 1. The open circuit voltages for freshly assembled cells were measured and are given in Table 2. The cells were discharged at constant currents of 30 mA (Comparative

Example 2a) and 6 mA (Comparative Example 2b) corresponding to C/3 and C/15 discharge rates, respectively. The gravimetric discharge capacities for cells discharged continuously at each of the rates to cutoff voltages of 1V and 0.8V also are given in Table 2. The values obtained for capacities to a 1V cutoff at both discharge rates were typically less than those for comparable cells of Example 1 having cathodes containing  $\lambda$ -MnO<sub>2</sub> prepared from Spinel B and discharged at corresponding rates. The capacity of cells discharged to a 0.8V cutoff at a C/15 rate also was somewhat lower for cells having cathodes containing the  $\lambda$ -MnO<sub>2</sub> prepared from Spinel A.

Table 2

Ex. No.	Cathode Matl	Vacuum Filled	Discharge Rate	Ave OCV (V)	Capacity to 1V (mAh/g)	Capacity to 0.8V (mAh/g)
C1b	EMD	No	C/15	1.60	245	266
C2b	$\lambda$ -MnO <sub>2</sub>	No	C/15	1.69	204	290
1b	$\lambda$ -MnO <sub>2</sub>	No	C/15	1.65	220	302
1d	$\lambda$ -MnO <sub>2</sub>	Yes	C/15	1.68	206	289
C1a	EMD	No	C/30	1.61	262	282
1a	$\lambda$ -MnO <sub>2</sub>	No	C/30	1.65	233	312
C1c	EMD	No	C/3	1.6	164	215
C2a	$\lambda$ -MnO <sub>2</sub>	No	C/3	1.69	159	218
1c	$\lambda$ -MnO <sub>2</sub>	No	C/3	1.66	167	187

10

The average OCV values for cells containing  $\lambda$ -MnO<sub>2</sub> prepared from the Spinel A and B ranged from 1.64 to 1.69 V compared to a value of about 1.60 to 1.62 V for cells containing a commercial EMD (e.g., Kerr-McGee Trona D EMD). The discharge capacities to 1V and 0.8V cutoffs are shown in Table 2. The values given are the averages for 4-5 individual button cells.

15

The capacity to a 0.8 V cutoff for cells with cathodes containing  $\lambda$ -MnO<sub>2</sub> prepared from Spinel B discharged at a C/30 rate was nearly 110% that for button cells with cathodes containing commercial EMD to a 0.8 V cutoff. Further, the discharge capacity to a 0.8 V cutoff for cells with cathodes containing  $\lambda$ -MnO<sub>2</sub> prepared from Spinel B discharged at a C/15 rate was nearly 113% that for cells with cathodes containing commercial EMD. However, the discharge capacity to a 0.8V cutoff for cells with cathodes containing  $\lambda$ -MnO<sub>2</sub> prepared from Spinel A discharged at a C/15 rate was about 110% that for cells with cathodes containing EMD and only

20

about 95% for cells with cathodes containing  $\lambda$ -MnO<sub>2</sub> prepared from Spinel B. The capacity to a 0.8 V cutoff for cells with cathodes containing  $\lambda$ -MnO<sub>2</sub> prepared from Spinel A discharged at a C/3 rate was nearly identical to that for cells with cathodes containing commercial EMD.

The incremental discharge capacity and maximum power,  $P_{max}$ , for an alkaline button cell 5 having a cathode containing  $\lambda$ -MnO<sub>2</sub> of Example 1 were determined for a cell discharged to a cutoff of about 0.75V by SPECS and the results depicted in Figure 4. The Stepped Potential Electro-Chemical Spectroscopy (viz., SPECS) method has been disclosed in ITE Letters on Batteries, Vol. 1, No. 6, 2000, pp. 53-64, which is incorporated herein by reference in its 10 entirety. Although the peaks centered at about 1.25V and 1.12V are observed commonly for commercial EMD materials, the additional broad peaks centered at about 1.55V and 0.95V in both curves denote the contributions of incremental capacity and maximum power from discharge processes that typically are not observed for a commercial EMD. The incremental 15 discharge capacity and maximum power for an alkaline button cell (Comparative Example 1) discharged to a cutoff of about 0.9V with a cathode containing commercial EMD from Kerr-McGee (e.g., Trona-D) also were determined by SPECS and the results depicted in Figure 5. By comparison, the commercial EMD exhibited broad peaks near 1.45V and 1.3V and the absence 20 of the peaks near 1.55V and 0.95V that are characteristic of  $\lambda$ -MnO<sub>2</sub>. Thus, the presence of these latter peaks indicate the particular suitability of the  $\lambda$ -MnO<sub>2</sub> cathode material of this invention for use in high-energy, high-capacity primary alkaline cells.

Furthermore, the broad peaks near 0.95V in both the incremental capacity and the 25 maximum power plots for a typical commercial EMD (See Figure 5) can be attributed to the further reduction of groutite,  $\alpha$ -MnOOH, the initial one-electron reduction product, to the final two-electron reduction product, pyrochroite, Mn(OH)<sub>2</sub>. The electrochemical two electron reduction of  $\gamma$ -MnO<sub>2</sub> to Mn(OH)<sub>2</sub> has been studied extensively (See, for example, A. Kozawa, in "Batteries, Vol. 1, Manganese Dioxide," K.V. Kordesch, ed., New York: Marcel Dekker, Inc., 1974, pp. 385-515) and has been shown to proceed by a two step reduction process involving an initial solid state proton insertion during the first electron reduction followed by dissolution and precipitation during the second electron reduction (See, R. Patrice *et al.*, ITE Batteries, Vol. 2, No. 4, 2001, ppB6-14). Further, it was revealed that  $\gamma$ -MnO<sub>2</sub> provides very little discharge 30 capacity from the second electron reduction in alkaline cells having relatively low levels of conductive carbon particles in the cathode, carbon particles with low surface area, high

concentrations of KOH in the electrolyte solution or zinc oxide present in the electrolyte. As a result, the reduction of groutite to pyrochroite typically is disfavored for consumer manganese dioxide/zinc alkaline primary cells and thus, very little additional discharge capacity is obtained below about 0.9V. Under identical discharge conditions, cells having cathodes containing  $\lambda$ -MnO<sub>2</sub> provide substantial additional capacity at about 0.95V as shown in the incremental capacity plot in Figure 4. In fact, a quantitative study of this incremental capacity plot reveals the specific capacity of the  $\lambda$ -MnO<sub>2</sub> of Example 1 is about 220 mAh/g before including the contribution of the additional capacity resulting from the second electron reduction process at 0.95V and about 320 mAh/g when it is included. This represents a contribution of about 100 mAh/g or about 30% of the total discharge capacity that can be attributed directly to the second electron reduction process in the case of cells containing  $\lambda$ -MnO<sub>2</sub>. However, the detailed reaction mechanism for the electrochemical two-electron reduction process for  $\lambda$ -MnO<sub>2</sub> has not yet been determined.

#### EXAMPLE 2

A sample of dried  $\lambda$ -MnO<sub>2</sub> powder was prepared as described in Example 1. The  $\lambda$ -MnO<sub>2</sub> powder was blended using a high-speed laboratory mixer mill (e.g., Waring mixer) with a natural graphite (Nacionale de Grafite, MP-0702X) and 38% KOH electrolyte solution in a weight ratio of 87:8:5.

Button cells having cathodes containing this cathode mix were fabricated in the same manner as in Example 1. The open circuit voltages for freshly assembled cells were measured and are listed in Table 3. The cells were discharged at constant currents of 3 mA (Example 2a) and 30 mA (Example 2b) corresponding to C/40 and C/4 discharge rates, respectively. The C/40 and C/4 discharge rates correspond to 7 mA/g of active cathode material and 70 mA/g of active cathode material. The gravimetric discharge capacities for cells discharged continuously at each of the constant current values to cutoff voltages of 1V and 0.8V also are given in Table 3. The values of capacities to 1V obtained for both discharge rates were nearly identical to those obtained for comparable cells having cathodes containing EMD instead of  $\lambda$ -MnO<sub>2</sub> and discharged at corresponding rates. The values of capacities for cells discharged to 0.8V at both rates were slightly lower than those obtained for comparable cells having cathodes containing EMD instead of  $\lambda$ -MnO<sub>2</sub> (See Comparative Example 2).

EXAMPLE 3

5 A sample of dried  $\lambda$ -MnO<sub>2</sub> powder was prepared as described in Example 1. The  $\lambda$ -MnO<sub>2</sub> powder was blended using a high-speed laboratory mixer mill (e.g., Waring mixer) with an admixture containing a 1:1 weight ratio of a natural graphite (Nacionale de Grafite, MP-0702X) and an expanded graphite (Timcal, EBNB-90) and 38% KOH electrolyte solution in an overall weight ratio of 87:4:4:5.

10 Button cells having cathodes containing this cathode mix were fabricated in the same manner as in Example 1. The open circuit voltages for freshly assembled cells were measured and are listed in Table 3. The cells were discharged at constant currents of 3mA (Example 3a) and 30 mA (Example 3b) corresponding to C/40 and C/4 discharge rates, respectively. The C/40 and C/4 discharge rates correspond to 7 mA/g of active cathode material and 70 mA/g of active cathode material. The gravimetric discharge capacities for cells discharged continuously at each of the constant current values to cutoff voltages of 1V and 0.8V also are given in Table 3. The average capacity for cells discharged to 0.8V at a C/40 rate was about 111% that for comparable 15 cells having cathodes containing EMD instead of  $\lambda$ -MnO<sub>2</sub> and discharged at the same rate (see Comparative Example 2).

COMPARATIVE EXAMPLE 3

20 EMD (Kerr-McGee Trona D) powder was blended using a high-speed laboratory mixer mill (e.g., Waring mixer) with an admixture containing a 1:1 weight ration of a natural graphite (Nacionale de Grafite, MP-0702X) and an expanded graphite (Timcal, EBNB-90) and 38% KOH electrolyte solution in an overall weight ratio of 87:4:4:5.

25 Button cells were fabricated as in Example 1. The open circuit voltages for freshly assembled cells were measured and are listed in Table 3. The cells were discharged at constant currents of 3mA (Comparative Example 3a) and 30 mA (Comparative Example 3b) corresponding to C/40 and C/4 discharge rates, respectively. The gravimetric discharge capacities for cells discharged continuously at each of the constant current values to cutoff voltages of 1V and 0.8V are given in Table 3.

Table 3

Example No.	Active Cathode Matl	Total Graphite Level (wt%)	Discharge Rate	Ave OCV (V)	Capacity to 1V (mAh/g)	Capacity to 0.8V (mAh/g)
C3a	EMD	4+4	C/40	1.62	207	237
3a	$\lambda$ -MnO <sub>2</sub>	4+4	C/40	1.71	203	263
2a	$\lambda$ -MnO <sub>2</sub>	8	C/40	1.73	196	220
C3b	EMD	4+4	C/4	1.62	144	156
2b	$\lambda$ -MnO <sub>2</sub>	4+4	C/4	1.73	125	130
3b	$\lambda$ -MnO <sub>2</sub>	8	C/4	1.73	142	146

A number of embodiments of the invention have been described. Nevertheless, it will be understood that various modifications may be made without departing from the spirit and scope

5 of the invention. For example, oxidative delithiation of the precursor spinel can be performed using a variety of aqueous oxidizing agents including, for example, an aqueous solution of sodium or potassium peroxydisulfate, sodium or potassium peroxydiphosphate, sodium perborate, sodium or potassium chlorate, sodium or potassium permanganate, cerium (+4) ammonium sulfate or nitrate, or sodium perxenate, or ozone gas bubbled through acidic water.

10 Non-aqueous oxidizing agents include, for example, nitrosonium or nitronium tetrafluoroborate in acetonitrile, nitrosonium or nitronium hexafluorophosphate in acetonitrile, or oleum (i.e., SO<sub>3</sub>/H<sub>2</sub>SO<sub>4</sub>) in sulfolane. Using an aqueous chemical oxidant such as peroxydisulfate, ozone or a non-aqueous oxidizing agent to oxidize the Mn<sup>+3</sup> ions to Mn<sup>+4</sup> ions in the LiMn<sub>2</sub>O<sub>4</sub> spinel can result in substantially less manganese being lost by dissolution than in the disproportionation process (Equation 1) taking place during treatment with an aqueous acid solution.

15 Other embodiments are within the claims.